

Research Article

Microwave Reduced Graphene Oxide as Efficient NIR Photothermal Agent

Sunayana Kashyap¹, Vinod Kumar², Shiju Abraham³, Sima Umrao³, Siddharath Singh⁴, Arpana Kamath⁵, Rajala MS⁵, Anchal Srivastava³ and Preeti S Saxena^{1*}

¹Department of Zoology, Banaras Hindu University, India

²Institute of Nanoscience & Technology, India

³Department of Physics, Banaras Hindu University, India

⁴Department of Biotechnology, G.B. Pant Engineering College, India

⁵School of Biotechnology, Jawaharlal Nehru University, India

*Corresponding author: Preeti S Saxena, Department of Zoology, Banaras Hindu University, Varanasi-221005, India

Received: April 10, 2017; Accepted: May 22, 2017;

Published: June 07, 2017

Abstract

Current study reports the enhanced cancer cells photothermal ablation efficiency of Microwave Reduced Graphene Oxide (MRGO). Reduction of chemically exfoliated graphene oxide has been carried out using a microwave (700W for 5 minutes). The produced MRGO have been characterized with TEM, SEM, XRD, FTIR, RAMAN, AFM and UV-Vis spectroscopy. MRGO nano size sheets with average lateral dimension ~200nm, exhibited higher NIR absorption efficiency, in comparison to Graphene Oxide (GO). Photothermal efficacy (at optimized NIR laser 808 nm, power of 5.0W/cm² for 5 min) of MRGO have been tested against human alveolar epithelial carcinoma cell (A549) and human colorectal carcinoma cells (HCT116). As a result, a significant decrease in cell viability by 84% and 80% for A549 and HCT116 cell lines respectively has been estimated. No significant toxicity has been observed with MRGO (in absence of NIR treatment) at the concentrations well above the doses needed for photothermal heating against the same cancer cells. Our study introduces MRGO as a biocompatible and efficient photothermal agent.

Keywords: Photothermal therapy; Microwave assisted reduced graphene oxide; A549 and HCT116 cancerous cells

Introduction

Cancer is the leading cause of death worldwide. Around 14.1 million cases of cancer were found in the world in which 7.4 million were of men and 6.7 million of women in 2012 and it is expected this number can increase to 24 million till 2035 [1]. More than 200 types of cancer have been reported. Out of these, lung and colorectal cancer are the serious concern to both developed as well as developing countries. Lung cancer is the most frequently diagnosed cancer (1.61 million, 12.7% of the total) while, colorectal cancer is the third most common causes of cancer death (1.23 million, 9.7% of the total) [2]. There are several means for the treatment of cancer such as surgery, chemotherapy, radiotherapy, and sometimes a combination of them. But each of them suffers with certain drawbacks such as severe adverse reactions, low efficiency and occurrence of other health complications [3-6]. In past decades, photothermal therapy using near-infrared spectrum of light employing a photothermal agent has emerged as an alternative and effective tool for photo ablation of cancer cells with minimum side effects to nearby healthy cells [7-10].

In recent years, 2-D carbon nanomaterials i.e. Graphene Oxide (GO) and Reduced Graphene Oxide (RGO) owing excellent physicochemical properties, have been widely explored for NIR mediated photothermal ablation of cancer cells [11,12]. However, the issue of inherent toxicity of RGO acquired through the utilization of toxic reducing agents remains a matter of debate [12]. Up to now, in most of biomedical applications Chemically Reduced Graphene Oxide (CRGO) have been used. In chemical reduction of GO, several non-ecofriendly reducing agent like hydrazine hydrate, its derivatives like dimethyl hydrazine and various metal hydrides, e.g. sodium hydride, sodium borohydride (NaBH₄) and Lithium Aluminium Hydride (LiAlH₄) have been employed [13]. These chemical reducing

agents are generally toxic in nature and not efficient for complete reduction of all functional groups present over GO. For e.g. NaBH₄ effectively reduces only C = O rather than epoxy groups, carboxylic acids groups and alcohol groups [14]. Usually RGO is obtained by graphene oxide reduction at high temperature, or by use of reducing agent [15]. Reduction of GO by unconventional heating resources as microwave irradiation is better alternative over the popular chemical reduction methods. It facilitates quick, inexpensive and mass production of RGO with little energy cost, overcoming the problems associated with chemically reduced RGO [16-18]. Further in the best of our knowledge, no reports are available towards the biomedical application of MRGO. In the current study, an attempt have been made to exploit the enhanced NIR absorption efficiency of MRGO for photothermal destruction of human alveolar epithelial carcinoma cell (A549) and human colorectal carcinoma cells (HCT116). This is the first study which reports the photothermal application of MRGO.

Experimental Details

Materials

Graphite flakes were obtained from NGS Naturgraphit GmbH (Germany). H₂SO₄, H₃PO₄ and all other chemicals were purchased from Merck limited, Mumbai, India. All the chemical reagents were of analytical grade.

Synthesis of graphene oxide (GO)

GO have been synthesized by improved Hummers method with a slight modification [19,]. In brief, 1 g of graphite powder have been pre-oxidized by reacting it with a mixture of 40 ml of 98% H₂SO₄, 5g K₂S₂O₈ and 5 g of P₂O₅ for 4h at 80°C. Further oxidation have been achieved by adding the pre-oxidized graphite to a mixture of concentrated H₂SO₄-H₃PO₄ (v/v: 180: 13) with constant stirring.

After 5 min, 6 g of KMnO_4 have been added to the mixture and the stirring is continued for 15 h at 55°C . The reaction is stopped and the reactants were allowed to cool at RT followed by pouring of 200 ml of ice and 1.5 ml of H_2O_2 (30%). Multiple washings of the material have been carried out with DI water, 30% HCl and ethanol and finally coagulated with ether. The obtained semi-solid material has been vacuum dried overnight to obtain brown Graphene Oxide (GO) powder.

Reduction of graphene oxide (GO)

Reduced Graphene Oxide (RGO) has been obtained by reduction of Graphene Oxide (GO) by microwave reduction method. In microwave reduction, 100 mg of GO powder (kept in 250 ml conical flask) was irradiated with 700 W of microwaves for 5 minute (using a domestic microwave oven). The exfoliation of GO layers takes place and fluky lightweight MRGO was obtained (Figure S3).

Characterization

Transmission electron microscopy (TEM, Tecnaii-G2F30 STWIN), operated at an accelerating voltage of 200 KeV and scanning electron microscopy (SEM, JEOL-Model JSM6300F) have been used for structural characterization of GO and MRGO. The UV-Visible absorbance spectra of GO and MRGO solutions were recorded with Perkin Elmer UV-Visible-Lambda 25 spectrophotometer. FTIR and Raman spectrum have been recorded using Thermo scientific Fourier transform infrared spectroscopy (Thermo Nicolet-6700) and FT-Raman by Perkin Elmer Spectrum Raman instrument. The X-ray diffraction (XRD, Rigakuminiflex-II diffractometer at 30 kV, 15mA) was used to find the diffraction patterns of GO and MRGO (at wavelength of radiation $\text{Cu-K}\alpha 1 \sim 1.5405\text{\AA}$). AFM image was recorded by (Nanosurf Model: Easy scan 2 with scan rate of 0.5.Hz. Cellular imaging was done using a Primo vert Zeiss microscope. Hemocytometer-Superior Marienfeld Germany Plate Reader-TECAN Austria Gmb, Model-Sunrise Basic Tecan.were used for cell counting and cell viability assay.

Cell culture

Human Colorectal carcinoma cells (HCT116 cells) and human alveolar epithelial carcinoma cells. (A549 cells) were cultured separately in a 25cm^2 tissue culture flask with Dulbecco's Modified Eagle Medium (DMEM) and Ham's F12 containing 10% FBS (Fetal Bovine serum) 20mM D-glucose, penicillin (100 units/mL), and $100\mu\text{g/mL}$ streptomycin. Cells were allowed to grow in a humidified condition at 37°C and 5% CO_2 atmosphere.

Cytotoxicity evaluation

3-(4, 5-dimethylthiazol-2-yl)-2, 5-diphenyl tetrazolium bromide (MTT) assays was carried out to evaluate the cytotoxic effects of MRGO against both A549 cells and HCT116 cells. For this, cells were cultured and maintained in DMEM and Ham's F12 medium, 5000 cells/well were seeded in 96 wells plates. Different concentrations (such as 0, 5, 10, 20, 50, 100 and $200\mu\text{g/mL}$) of MRGO were added in separate wells followed by 24 hours of incubation at 37°C with 5% CO_2 atmosphere. Each concentration was added in triplicates. After 24 hours of incubation $20\mu\text{L}$ of 5.0 mg/mL MTT was added in each well and incubated for 4 hours, there after $200\mu\text{L}$ of DMSO was added to solubilize the resultant formazan crystals. Optical density was measured at 590-610 nm. The cell viability was estimated according

to the following equation:

$$\text{Cell Viability [\%]} = (\text{OD treated} / \text{OD control}) \times 100\%$$

Where, OD control was absorbance value estimated from cells without incubation of MRGO and OD treated was absorbance estimated in the presence of MRGO.

NIR mediated phototherapy

NIR laser (Nd:YAG) of 808 nm with 5.0 W/cm^2 of power density was used for phototherapy experiment. 5000 of each kind of cells/wells (A549 cells and HCT116) were seeded in 96 well plates in six different groups in triplicate separately. In first group, normal cell (without MRGO) with no laser treatment were taken. In second group, cells (without MRGO) after laser treatment were taken. The third group consists of cells with $15.0\mu\text{g/mL}$ MRGO without laser treatment. The fourth, fifth and sixth group consist of cells with $15.0\mu\text{g/mL}$ MRGO exposed by NIR laser with different time interval as 2.0, 3.0 and 5.0 minutes respectively. After the NIR irradiation cells were washed with PBS (pH-7.4) and cell viability was estimated with trypan blue exclusion method.

Statistical analysis

Statistical analysis were done with SPSS-16 software using One way ANOVA and significant difference of means were determined using Duncan's multiple range test at the level of $p < 0.05$ and $p < 0.001$.

Results and Discussion

Structural characterization of MRGO has been carried out using Atomic Force Microscope (AFM), Scanning Electron Microscopy (SEM) and Transmission Electron Microscopy (TEM). The AFM image (Figure 1A) of MRGO showed uniform larger sheet with lateral dimension of 500 nm and average height profile of $\sim 90\text{nm}$, which has been reduced significantly i.e upto $\sim 200\text{ nm}$ by ultra-sonication (Figure S1A) supporting information). The ultrasonicated MRGO sheets with $\sim 200\text{ nm}$ of lateral dimension have been further used for photothermal experiments. The average height profile of the MRGO nanosheets has been found to be $\sim 40\text{nm}$ (Figure S1.B supporting information). Well-exfoliated but crumpled and aggregated MRGO sheets are observable in the SEM image (Figure 1B) which is a

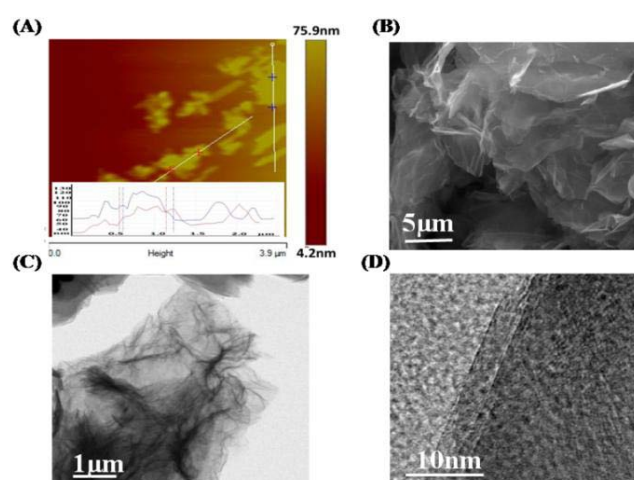


Figure 1: (A) AFM image of MRGO (B) SEM image of MRGO (C) TEM image of MRGO (D) HRTEM image of MRGO.

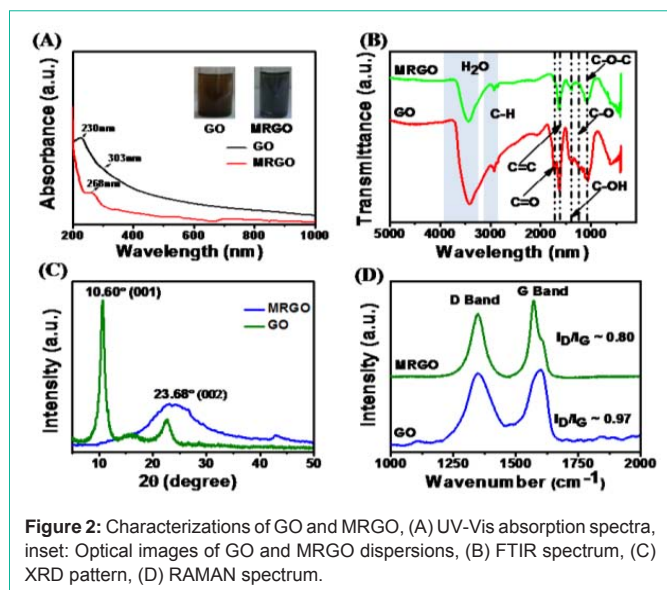


Figure 2: Characterizations of GO and MRGO, (A) UV-Vis absorption spectra, inset: Optical images of GO and MRGO dispersions, (B) FTIR spectrum, (C) XRD pattern, (D) RAMAN spectrum.

common feature of the RGO. TEM image of the MRGO (Figure 1C) shows the wrinkled structure of folded sheet with lateral dimension of $\sim 1\mu\text{m}$ which break up into small sheet sizes with lateral dimension around $\sim 200\text{ nm}$ after ultrasonication (Figure S2). Thus the results obtained in TEM image are in well agreement with the observation made in AFM. HRTEM (Figure 1D) of MRGO indicates its crystal and few layered nature [20,21].

In Figure 2A shows the UV-Vis absorption spectrum of GO and MRGO (Inset picture show the optical image of GO and MRGO Figure 2A). The absorption peak at 230 nm is due to $\pi-\pi^*$ transition of aromatic C-C bonds which is red shifted to 268 nm, indicating the electronic conjugation within the reduction of GO by exfoliation of GO layers due to microwave irradiation [22]. The RAMAN spectrums of as synthesized GO and MRGO were shown in Figure 2D. The GO and MRGO show G-band due to C-C vibration with sp^2 carbon which corresponds to the E_g^2 phonon at the centre of the Brillouinzone and D-band (sp^3 carbon) comes from the out-of-plane breathing mode of the sp^2 carbons, which is due to the presence of defects that were introduced in oxidization and reduction procedure. In case of GO, the G band was at 1571.7 cm^{-1} , while in case of MRGO the G band shifted to 1600.5 cm^{-1} . This indicated the reduction of GO is happening by exfoliation of layered structures of GO under microwave irradiation. The D band for GO and MRGO was sited at 1349 cm^{-1} and 1347 cm^{-1} respectively. In case of MRGO, the I_D/I_G ratio was 0.80, which was smaller than the I_D/I_G ratio of GO. The reduced I_D/I_G value was attributed to the removal of defects originated due to oxygen containing functional groups and the conversion of sp^3 to sp^2 carbon [23].

In the FT-IR spectrum of the GO (Figure 2B), the peaks at, $3432, 1720, 1410, 1245$ and 1045 cm^{-1} were attributed to O-H, C=O stretch of COOH, C-OH, C-O and C-O-C bands, respectively. The absorption peaks at 2930 cm^{-1} and 2850 cm^{-1} show the symmetric and anti-symmetric stretching vibrations of C-H, while the presence of two absorption peaks observed at 1630 cm^{-1} can be attributed to the stretching vibration of C=C. Upon the exfoliation of GO by microwave irradiation, the C=O bands disappear and intensity of

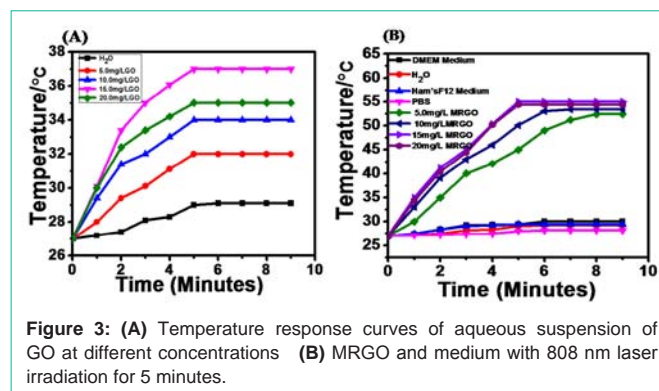


Figure 3: (A) Temperature response curves of aqueous suspension of GO at different concentrations (B) MRGO and medium with 808 nm laser irradiation for 5 minutes.

C-H stretching band increase. In the FTIR spectrum of MRGO (Figure 2B), the intensity of -OH vibrations observed at 3400 cm^{-1} is significantly reduced due to deoxygenation but it confirmed the presence of carboxylic functional group [24].

The powder X-Ray Diffraction (XRD) pattern (CuK α radiation) measurements were carried out to investigate the phase and structure of as synthesized RGO. In the XRD pattern of the GO (Figure 2C), a sharp peak at 10.60° , corresponding to reflection of (001) plane (interlayer spacing of 0.83 nm) and the other one less intense peak at 22.12° was shown corresponding to (002) plane. After microwave reduction of GO, the sharp (002) peak of GO disappeared while another broad peak of around 23.68° shows up. The disappearance of the sharp peak in MRGO can be attributed to the exfoliation of layered structures of GO under microwave irradiation and the broad peak at 23.68° with interlayer spacing of 0.37 nm may originate from the partial restacking of exfoliated graphene layers [24].

The temperature response curves measured at different time points with different concentration of GO and MRGO after irradiating laser at 808 nm (5.0 W/cm^2) are shown in Figure 4. The laser irradiation effect (for 5 minutes) with the varying concentration of GO like 5.0 mg/L, 10.0 mg/L, 15.0 mg/L and 20.0 mg/L leads to rise in temperature as 32°C , 34°C , 37°C and 35°C respectively (Figure 3A). In contrast under same set of condition the temperature rise in case of MRGO was noticed to be 45°C , 50.1°C , 55°C and 54.4°C respectively (Figure 3B). DMEM media, Ham's12 media, Phosphate-Buffered Saline (PBS) and water did not show any response to the irradiation even at 5.0 W/cm^2 . The above observations suggest the superior photothermal heating property in MRGO in comparison to GO.

Cytotoxic effect of MRGO on A549 and HCT116 cells were evaluated by MTT [3-(4,5-dimethylthiazol-2-yl)-2,5-diphenyl tetrazolium bromide] assays, result of which were shown in Figure 4A and B. Up to $200\mu\text{g/mL}$ concentration of MRGO, no significant toxicity has been estimated for both A549 cells and HCT116 cells, which describe the good biocompatibility of MRGO. The statistical analysis of the result was done by One way ANOVA followed by Duncan's test at the level of $p < 0.05$. Cytotoxicity results reveal that there is no significant difference in the biocompatibility of MRGO and CRGO.

The photothermal effect of MRGO against A549 and HCT 116 cells were studied with the help of try pan blue exclusion method and

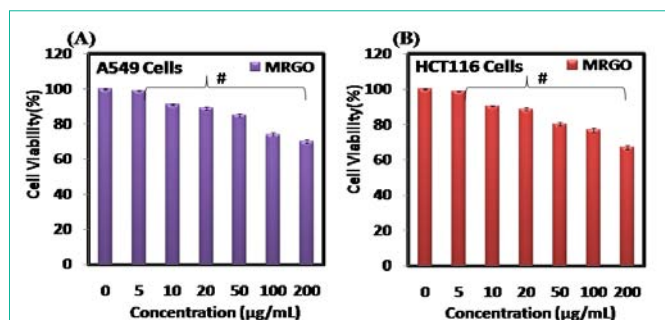


Figure 4: (A) MTT based colorimetric assay graph for cell viability of A549 cells and (B) HCT116 cells incubated for 24 hours with different concentration of MRGO as (0, 5, 10, 20, 50, 100 and 200 µg/mL). The statistically not significant values are labelled with # at ($p > 0.05$).

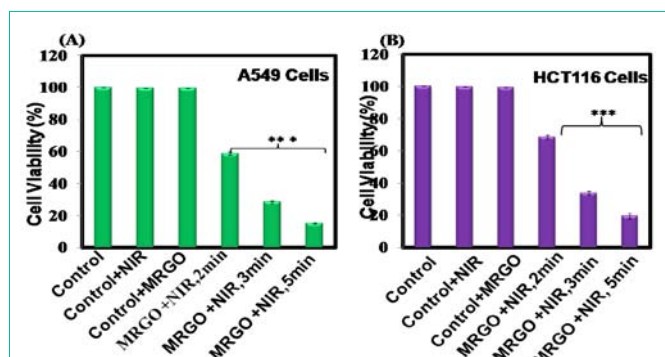


Figure 5: (A) Cell viability of A549 cells and (B) HCT116 cells after exposure of NIR laser (808 nm, 5.0 W/cm²) at different time interval of 0, 2, 3, 5 min with 15 µg/mL concentration of MRGO. The statistically significant values is labelled by * at ($p < 0.05$).

the results were shown in Figure 5A and B. Percentage decrease in cell viability was calculated as 41%, 72% and 84% for A549 cells and 31.0%, 67% and 80% for HCT116 after 2.0, 3.0 and 5.0 minutes of NIR irradiation in the above cell suspensions containing MRGO. Further, negligible decrease in cell viability *i.e.* 99.6% and 99.4% for HCT116 and A549 cells respectively have been noticed after NIR irradiation for 5 minutes without MRGO in cell suspensions. Moreover, almost no decrease in cell viability *i.e.* 99.2% and 99.5% for HCT116 and A549 respectively was observed when only MRGO was incubated with cell for 5 minutes. The cell viability results shown above were calculated and were in respect of control cell's viability which was 100%.

After photothermal treatment mediated by MRGO both A549 and HCT116 were stained with trypan blue and further examination was made under light microscope (Figure 6 and 7). The cells with only MRGO (Figure 6C and 7C) and treated with NIR (Figure 6B and 7B), did not show any uptake the blue colour of trypan dye like control cells (Figure 6A and 7A) which indicates that all the cells were viable, and this is because neither NIR laser nor MRGO itself may have potential to induce severe cell death. However, the presence of MRGO in cell suspension coupled with NIR radiation causes cell death which increases with time of irradiation for both kind of cells. Several blue stained dead cells appeared (Figure 6D and 7D) after 2 minute exposure of laser with MRGO treatment with preponderance of live cells, on the other hand almost all cells were blue stained 5.0 minutes of exposure (Figure 6E, F and 7E, F). Moreover, morphological

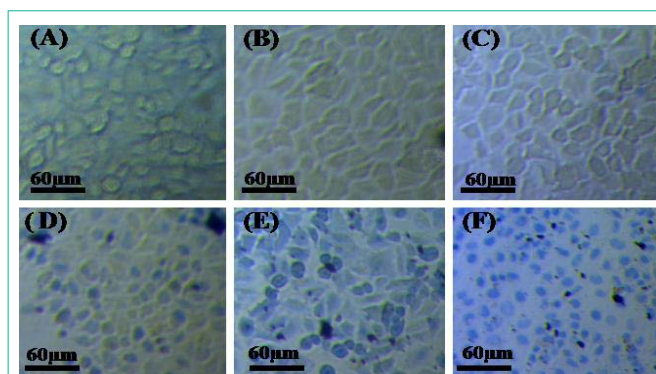


Figure 6: (A) Optical images of A549 Control cells, (B) Control cells after laser irradiation, (C) Cells with 15.0 µg/mL MRGO, (D) Cells with 15.0 µg/mL MRGO after 2 minutes of laser irradiation (5.0W/cm², 808 nm), (E) after 3 minutes of laser irradiation, (F) after 5 minutes of laser irradiation. Blue colour indicates dead cells (Trypan blue test). Scale bar = 60 µm.

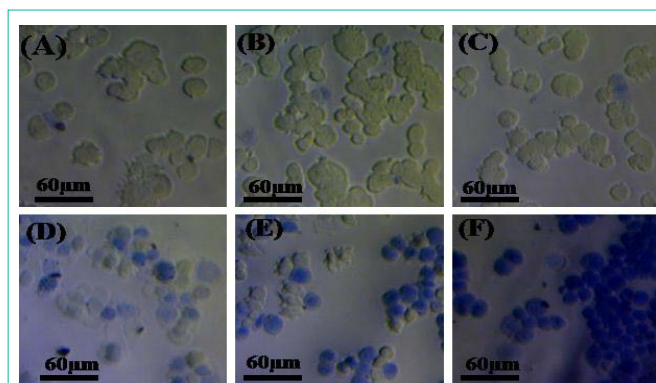


Figure 7: (A) Optical images of HCT 116 Control cells, (B) Control cells after laser irradiation, (C) Cells with 15.0 µg/mL MRGO, (D) Cells with 15.0 µg/mL MRGO after 2 minutes of laser irradiation (5.0W/cm², 808 nm), (E) after 3 minutes of laser irradiation, (F) after 5 minutes laser irradiation. Blue colour indicates dead cells (Trypan blue test). Scale bar = 60 µm.

changes can also be seen in microscopic examination of the cells with MRGO after NIR exposure.

In the current, study we could not explore the exact mechanism of cell death but it may be due to protein denaturation and coagulation as well as membrane destruction, which is primarily due to thermal disintegration up to 55°C expansion during NIR mediated phototherapy of MRGO. MRGO have shown better photothermal effect at lower laser power density *i.e.* 5.0W/cm² in comparison to other nanomaterial based photothermal agent such as gold nano shell, and nanorod, which require high power density such as 35.0 W/cm² and 10.0W/cm² respectively [25, 26]. Further, study is underway to explore the mechanism of cell death and *in-vivo* application.

Facile and quick microwave assisted synthesis of MRGO with its high potential as photothermal agent will be an alternative therapeutic means for cancer therapy.

The high near infra-red absorption property of MRGO is solely attributed to the microwave assisted reduction of GO into MRGO. In the current study, we could not explore the exact mechanism of high NIR efficiency of MRGO but we propose similar mechanisms reported earlier [27].

Conclusion

In summary, our study establishes Microwave Reduced Graphene Oxide (MRGO) as a biocompatible and efficient NIR photothermal agent. Microwave assisted reduction of graphene oxide create nearly removal of oxygen functional groups in MRGO. It is presumed that reduction of oxygen functional group in MRGO nano sheets facilitates high NIR absorption by MRGO. Hence, MRGO nanosheets with lateral dimension of ~200 nm exhibited enhanced photothermal effects at low power density in short time. Rapid and effective photothermal ablation of A549 and HCT 116 cancer cells by MRGO using NIR laser (808 nm at 5.0 W/cm² in 5 minutes) make it an interesting material for cancer phototherapy. The cost effective and ecofriendly production of MRGO with its high NIR absorption property can be further employed for *in vivo* photothermal application.

Acknowledgement

We are grateful to Prof. W. Kiefer University of Wurzburg (Germany) for gifting 808nm Laser. We acknowledge financial support from CAS program of Zoology Department, B.H.U., Varanasi and research fellowship from CSIR, New Delhi. Authors also acknowledge Biophysics laboratory, Department of Physics, B.H.U., Varanasi, for extending their laboratory facilities.

References

1. <http://globocan.iarc.fr> .2013.
2. Behera D. Epidemiology of lung cancer Global and Indian perspective. Journal Indian Academy of Clinical Medicine. 2012; 13: 131-137.
3. Schmid KE, Kornek GV, Scheithauer W, Binder S. Update on Ocular Complications of Systemic Cancer Chemotherapy. Survey of Ophthalmology. 2006; 51: 19-40.
4. Giordano SH, Kuo YF, Freeman JL, Buchholz TA, Hortobagyi GN, Goodwin JS. Risk of Cardiac Death After Adjuvant Radiotherapy for Breast Cancer. Journal of the National Cancer Institute. 2005; 97: 419-442.
5. Farrow DC, Hunt WC, Samet JM. Geographic variation in the treatment of localized breast cancer. The New England Journal of Medicine. 1992; 326: 1097-1101.
6. Polednak AP. Trends in and predictors of breast-conserving surgery and radiotherapy for breast cancer in Connecticut, 1988- 1997. International Journal of Radiation Oncology Biology Physics. 2002; 53: 157-163.
7. Moon HK, Lee SH, Choi HC. *In vivo* near-infrared mediated tumor destruction by photothermal effect of carbon nanotubes. ACS Nano. 2009; 3: 3707-3713.
8. Zhou F, Xing D, Ou Z, Wu B, Resasco DE, Chen WR. Cancer cell photothermal therapy in near infrared region by using single walled carbon nanotubes. Journal of Biomedical Optics. 2009; 14: 1-6.
9. Sherlock SP, Tabakman SM, Xie L, Dai H, Photothermally enhanced drug delivery by ultrasmall multifunctional FeCo/graphitic shell nanocrystals ACS. Nano. 2011; 5: 1505-1512.
10. Su Y, Wei X, Peng F, Zhong Y, Lu Y, Su S, et al. Gold nanoparticles-decorated silicon nanowires as highly efficient near-infrared hyperthermia agents for cancer cells destruction. Nano Letters. 2012; 12: 1845-1850.
11. Ghosh S, Dutta S, Gomes E, Carroll D, D'Agostino R, Olson J, et al. Increased heating efficiency and selective thermal ablation of malignant tissue with DNA-encased multiwall carbon nanotubes. ACS Nano. 2009; 3: 2667-2673.
12. Robinson JT, Tabakman SM, Liang Y, Wang H, Casalongue HS, Vinh D, et al. Ultrasmall reduced graphene oxide with near high near-infrared absorbance for photothermal therapy. Journal of the American Chemical Society. 2011; 133: 6825-6831.
13. Songfeng P, Hui-Ming C. The reduction of graphene oxide. Carbon. 2012; 50: 3210-3228.
14. Periasamy M, Thirumalaikumar M. Methods of enhancement of reactivity and selectivity of sodium borohydride for applications in organic synthesis. Journal of Organometallic Chemistry. 2000; 609: 137-151.
15. Gupta TK, Singh BP, Tripathi RK, Dhakate SR, Singh VN, Panwar OS, et al. Superior nano-mechanical properties of reduced graphene oxide reinforced polyurethane composites. RSC Advances. 2015; 5: 16921-16930.
16. Yang GH, Zhou YH, Wu JJ, Cao JT, Li L, Liu HY, et al. Microwave-assisted synthesis of nitrogen and boron co-doped graphene and its application for enhanced electrochemical detection of hydrogen peroxide. RSC Advances. 2013; 3: 22597-22604.
17. Yu H, Wang T, Wen B, Lu M, Xu Z, Zhu C, Chen Y, Xue X, Sun C, Cao M. Graphene/polyaniline nanorod arrays: synthesis and excellent electromagnetic absorption properties. Journal of Material Chemistry. 2012; 22: 21679.
18. Umrao S, Gupta TK, Kumar S, Singh VK, Sultania MK, Jung JH, et al. Microwave-Assisted Synthesis of Boron and Nitrogen co-doped Reduced Graphene Oxide for the Protection of Electromagnetic Radiation in Ku-Band. ACS Applied Materials Interfaces. 2015; 7: 19831-19842.
19. Marcano DC, Kosynkin DV, Berlin S, Sun JMA, Slesarev Z, Alemay A, et al. Improved synthesis of graphene oxide. ACS Nano. 2010; 4: 4806-4814.
20. Zhang H, Feng PX. Fabrication and characterization of few-layer graphene. Carbon. 2010; 48: 359-364.
21. Ortolani L, Cadelano E, Veronese GP, Boschi CD, Snoeck EE, Colombo L, et al. Folded graphene membranes: mapping curvature at the nanoscale. Nano Letters. 2012; 12: 5207-5212.
22. Thakur S, Karak N. Green reduction of graphene oxide by aqueous phytoextracts. Carbon. 2012; 50: 5331- 5339.
23. Thema FT, Moloto MJ, Dikio EDN, Kotsedi NN, Maaza LM, Khenfouch M. Synthesis and characterization of graphene thin films by chemical reduction of exfoliated and intercalated graphite oxide. Journal of Chemical Physics. 2012; 2013: 1-6.
24. Loryenyong V, Totepvimarn K, Eimburanaprat P, Boonchompoo W, Buasri A. Preparation and Characterization of Reduced Graphene Oxide Sheets via Water-Based Exfoliation and Reduction Methods. Advances in Materials Science and Engineering. 2013; 2013: 1-5.
25. Huang X, El-Sayed MA. Gold nanoparticles: Optical properties and implementations in cancer diagnosis and photothermal therapy. Journal of Advanced Research. 2010; 1: 13-28.
26. Loo C, Lin A, Hirsch L, Lee M, Barton J, Halas N, et al. Nanoshell-enabled photonics-based imaging and therapy of cancer. Technology in Cancer Research and Treatment. 2004; 3: 33-40.
27. Acik M, Lee G, Mattevi C, Chhowalla M, Cho K, Chabal YJ. Unusual infrared-absorption mechanism in thermally reduced graphene oxide. Nature Materials. 2010; 9: 840-845.